One-Axis Twisting as a Method of Generating Many-Body Bell Correlations

Marcin Płodzień,[1,*] Maciej Lewenstein,[1,2] Emilia Witkowska,[3] and Jan Chwedeńczuk[4]
[1]ICFO—Institut de Ciencies Fotoniques, The Barcelona Institute of Science and Technology, 08860 Castelldefels, Barcelona, Spain
[2]ICREA, Passeig Lluís Companys 23, 08010 Barcelona, Spain
[3]Institute of Physics PAS, Aleja Lotnikow 32/46, 02-668 Warszawa, Poland
[4]Faculty of Physics, University of Warsaw, ulica Pasteura 5, PL-02-093 Warsaw, Poland

(Received 27 June 2022; accepted 14 November 2022; published 16 December 2022)

We demonstrate that the one-axis twisting (OAT), a versatile method of creating nonclassical states of bosonic qubits, is a powerful source of many-body Bell correlations. We develop a fully analytical and universal treatment of the process, which allows us to identify the critical time at which the Bell correlations emerge and predict the depth of Bell correlations at all subsequent times. Our findings are illustrated with a highly nontrivial example of the OAT dynamics generated using the Bose-Hubbard model.

DOI: 10.1103/PhysRevLett.129.250402

Nonclassical correlations, namely entanglement and Bell correlations, are fundamental properties of the quantum many-body systems and crucial resources for emerging quantum technologies. Because of enormous challenges in fault-tolerant quantum computing, the main goal for quantum technologies in the next decade is to generate, characterize, validate, and certificate massively correlated quantum states [1–6]. To fully exploit many-body Bell correlations, we need an experimental protocol to generate such quantum states and a method for classifying the depth of many-body Bell correlations.

The well-known method for generating entangled states is the one-axis twisting (OAT), which has been used in various configurations and is a subject of extensive theoretical studies [7–16]. OAT can be realized with a variety of ultracold systems, utilizing atom-atom collisions [17–20] and atom-light interactions [21,22]. Theoretical proposals for the OAT simulation with ultracold atoms in optical lattices [23–28], effectively simulating Hubbard and Heisenberg models, are awaiting proof-of-principle experimental demonstration.

It is well understood that OAT creates many-body entangled states and the two-body Bell correlations inherent in two-body correlations [29,30]. An important question in the OAT procedure is about the generation of the many-body Bell correlated states. In [31–34], authors provide a set of Bell inequalities based on second-order correlators and show that their violation implies k producibility of nonlocality [35] with $k \leqslant 6$ for a large number of parties.

Here, we address the problem of nonlocality for an arbitrary depth k in the collection of qubits subject to the OAT procedure by employing a wide family of Bell inequalities using many-body correlators [36–42]. We analytically evaluate the many-body correlator providing a powerful formula allowing us to characterize the depth of many-body nonlocality at any moment of time. As such, we indicate the critical time at which the many-body Bell correlations emerge.

We begin with a brief outline of the OAT dynamics of N indistinguishable bosons. Each particle has two internal states a and b, with bosonic operators $\hat{a}$ and $\hat{b}$ annihilating a particle in a given state. The system is conveniently described by means of the collective angular momentum (spin) of length $j = N/2$, and the corresponding operators $\hat{J}_x = \frac{1}{2}(\hat{a}^\dagger\hat{b} + \hat{a}\hat{b}^\dagger), \hat{J}_y = (1/2i)(\hat{a}^\dagger\hat{b} - \hat{a}\hat{b}^\dagger), \hat{J}_z = \frac{1}{2}(\hat{a}^\dagger\hat{a} - \hat{b}^\dagger\hat{b})$ [43]. The OAT Hamiltonian reads

$$\hat{H}_{\mathrm{OAT}} = \chi \hat{J}_z^2, \tag{1}$$

where χ is an energy-unit constant [8]. The implementation of the OAT begins with a spin coherent state (CSS), $|(\pi/2), \varphi\rangle_{\mathrm{css}} = (1/\sqrt{N!})[(\hat{a}^\dagger + e^{i\varphi}\hat{b}^\dagger)/\sqrt{2}]^N|0\rangle$ being an eigenstate of $\hat{J}_x$ for $\varphi = 0$, $\hat{J}_x|(\pi/2), 0\rangle_{\mathrm{css}} = (N/2)|(\pi/2), 0\rangle_{\mathrm{css}}$. This state undergoes the dynamics

$$\hat{\varrho}(\tau) = \sum_{n,m=-\frac{N}{2}}^{\frac{N}{2}} c_n c_m^* e^{-i(n^2-m^2)\tau}|n\rangle\langle m|, \tag{2}$$

with the period equal to π for dimensionless $\tau = t\chi/\hbar$ for even N. Here, $|n\rangle$ is an eigenstate of $\hat{J}_z$, namely, $\hat{J}_z|n\rangle = n|n\rangle$ with $(N/2) - n$ bosons in mode a and $(N/2) + n$ in b, while $c_n = 2^{-N/2}\sqrt{\binom{N}{(N/2)+n}}$. For times $\tau \lesssim \tau_{\mathrm{s}}$, $\tau_{\mathrm{s}} \approx N^{-2/3}$ [8,44] the spin squeezing is generated, quantified by the squeezing parameter

$$\xi^2 = N\frac{\Delta^2\hat{J}_{\perp,\min}}{\langle\hat{J}\rangle^2}, \tag{3}$$

here, $\langle\hat{J}\rangle$ is the length of the mean collective spin and $\Delta^2\hat{J}_{\perp,\min} \equiv \langle\hat{J}^2_{\perp,\min}\rangle - \langle\hat{J}_{\perp,\min}\rangle^2$ is the minimal variance of

the collective spin orthogonally to its direction [45]. When ξ^2 drops below unity, it signals the presence of entanglement between the qubits and the potential metrological gain with respect to the standard quantum limit, namely, the sensitivity $\Delta\theta < 1/\sqrt{N}$ of estimation of some parameter θ.

At later times, $\tau > \tau_s$, the state enters a non-Gaussian regime. Though the time τ is a continuous variable, some particular instants $\tau_q = \pi/q$ labeled with integer $q = 2, 4, 6, \ldots$, are particularly important, because at these moments, a macroscopic superposition of coherent states [46,47]

$$|\psi_q\rangle = \frac{1}{\sqrt{q}} \sum_{k=0}^{q-1} e^{i\tau_q k(k+N)} \left| \frac{\pi}{2}, 2\tau_q k \right\rangle_{\mathrm{CSS}}, \tag{4}$$

is created. In particular, for $\tau_q = \pi/2$, a superposition of two coherent states is realized, forming the Schrödinger cat state.

To quantify the extent of many-body Bell correlations generated in the OAT process, we use a quantum (hence, labeled with the index "Q") N-body correlator $\tilde{\mathcal{E}}_N^{(Q)}$ which witnesses the Bell correlations if the inequality

$$\tilde{\mathcal{E}}_N^{(Q)} = \left| \frac{1}{N!} \langle \hat{J}_+^N \rangle \right|^2 \leqslant 2^{-N}, \tag{5}$$

is violated [42]. Here, $\hat{J}_+ = \hat{J}_1 + i\hat{J}_2$, where 1 and 2 denote any two orthogonal directions spanned by the triple operators $\{\hat{J}_x, \hat{J}_y, \hat{J}_z\}$. For the derivation of this bound, see Supplemental Material [48] and Refs. [37–39,42]. The average $\langle \hat{J}_+^N \rangle$ determines the coherence between the extreme elements of the density matrix, namely between $|-(N/2)\rangle$ and $|N/2\rangle$, where these two kets are the eigenstates of the operator orthogonal to directions 1 and 2.

Now, we discuss the main results of this Letter. A natural choice of the orientation of the plane spanned by the $\hat{J}_1$ and $\hat{J}_2$ operators is such that it maximizes the Bell correlator $\tilde{\mathcal{E}}_N^{(Q)}$. This, in turn, is determined by the OAT Hamiltonian (1) and the state (2). By inspecting Eq. (4), we notice that, at times τ_q, the OAT generates superpositions of eigenstates of $\hat{J}_x$ with varying weights and eigenvalues, depending on q. However, at $\tau_2 = (\pi/2)$ the NOON state is created, i.e.,

$$|\psi_2\rangle = \frac{1}{\sqrt{2}} \left(\left| \frac{N}{2} \right\rangle_x + \left| -\frac{N}{2} \right\rangle_x \right), \tag{6}$$

which is a macroscopic superposition of two states, the one state with N particles in mode a and the second state with N particles in mode b. Here, the subscript x denotes that the two components of the superposition are the eigenstates of $\hat{J}_x$ specifically. This observation, namely that the OAT procedure creates superpositions of eigenstates of $\hat{J}_x$, indicates that to detect most of quantum features of the OAT state, one should align 1 and 2 in the plane orthogonal to x. However, it is more convenient (and equivalent), to align 1 and 2 in the x-y plane and rotate the OAT state (2) around the y axis through angle $(\pi/2)$,

$$\hat{\varrho}_{\mathrm{rot}}(\tau) = e^{-i\frac{\pi}{2}\hat{J}_y} \hat{\varrho}(\tau) e^{+i\frac{\pi}{2}\hat{J}_y} = \sum_{n,m=-\frac{N}{2}}^{\frac{N}{2}} \tilde{\varrho}_{nm}^{(\tau)} |n\rangle\langle m|, \tag{7}$$

where the transformed element of the density matrix is

$$\tilde{\varrho}_{nm}^{(\tau)} = \sum_{n',m'=-\frac{N}{2}}^{\frac{N}{2}} d_{nn'}^{\frac{N}{2}} \left(\frac{\pi}{2} \right) d_{mm'}^{j} \left(\frac{\pi}{2} \right) \varrho_{n'm'}^{(\tau)}. \tag{8}$$

Here, $d_{\alpha\beta}^{j}(\phi)$ denotes the element of the Wigner rotation matrix [51].

After the rotation, the eigenstates of $\hat{J}_x$ transform into the eigenstates of $\hat{J}_z$ and the proper choice of the rising operator to maximize $\tilde{\mathcal{E}}_N^{(Q)}$ is $\hat{J}_+ = \hat{J}_x + i\hat{J}_y$, which gives

$$\tilde{\mathcal{E}}_N^{(Q)} = |\tilde{\varrho}_{-\frac{N}{2},\frac{N}{2}}^{(\tau)}|^2. \tag{9}$$

For the state (2), we obtain $\tilde{\varrho}_{-(N/2),(N/2)}^{(\tau)} = \tilde{C}_{-(N/2)}^{(\tau)} \tilde{C}_{(N/2)}^{(\tau)}$, where

$$\tilde{C}_{-\frac{N}{2}}^{(\tau)} = \frac{1}{2^N} \sum_{n=-\frac{N}{2}}^{\frac{N}{2}} \binom{N}{n+\frac{N}{2}} e^{-i\tau n^2}, \tag{10a}$$

$$\tilde{C}_{\frac{N}{2}}^{(\tau)} = \frac{1}{2^N} \sum_{n=-\frac{N}{2}}^{\frac{N}{2}} \binom{N}{n+\frac{N}{2}} (-1)^n e^{-i\tau n^2}, \tag{10b}$$

are the two coefficients of the state expressed in the basis of eigenstates of $\hat{J}_z$ with two extreme eigenvalues.

First, we focus on the short-time dynamics to identify the critical instant τ_{crit} at which the Bell correlations emerge in the OAT procedure, see Fig. 1(a) and 1(c). To this end, we notice that when τ is short, and N is large, the sums in Eq. (10) can be evaluated by approximating the binomial function with a Gaussian, namely,

$$\frac{1}{2^N} \binom{N}{n+\frac{N}{2}} \simeq \sqrt{\frac{2}{\pi N}} e^{-\frac{2}{N}n^2}, \tag{11}$$

which gives

$$\tilde{C}_{-\frac{N}{2}}^{\alpha} \simeq \frac{1}{\sqrt{1+i\kappa}}, \qquad \tilde{C}_{\frac{N}{2}}^{\alpha} \simeq 2\frac{e^{N\pi\frac{i(\kappa+\frac{\pi}{4})+1}{2(\kappa-i)}}}{\sqrt{1+i\kappa}}, \tag{12}$$

and the Bell correlator becomes

$$\tilde{\mathcal{E}}_N^{(Q)} \simeq \frac{4}{(1+\kappa^2)^2} e^{-\frac{\pi^2 N}{8(1+\kappa^2)}}, \tag{13}$$

with $\kappa = (\tau N/2)$. The τ_{crit} can be obtained by comparing the logarithm of $\tilde{\mathcal{E}}_N^{(Q)}$ with the logarithm of the threshold attainable by local realistic theories [see Eq. (5)], namely,

$$\ln 4 - 2\ln(1+\kappa^2) - \frac{\pi^2 N}{8(1+\kappa^2)} = -N \ln 2. \tag{14}$$

Note that, for large N, the two logarithms on the left-hand-side can be neglected giving the critical time at which the Bell correlations are created in the OAT procedure [52]

$$\tau_{\text{crit}} \simeq \frac{2}{N}\sqrt{\frac{\pi^2}{8\ln 2} - 1} \approx \frac{1.77}{N}. \tag{15}$$

It is worth stressing here that the Bell correlations emerge before optimal squeezing time as $\tau_{\text{crit}} < \tau_s$ in the large N limit. At the instant τ_{crit}, three particles are Bell correlated, the smallest minimal number for which the correlator (5) exceeds the local bound [40].

At later times, the continuous approximation fails, as it cannot capture the genuinely quantum discrete-N interference phenomena, see Fig. 1(a) and 1(c). A close analogy is the series of collapses and revivals in the two-level dynamics of an atom driven by quantized coherent electromagnetic fields [53], which are not captured by the semiclassical approach.

However, this is when the result of Eq. (4) comes at hand. At instants τ_q, when superpositions of coherent states (4) are formed, the two extreme coefficients can be calculated analytically, giving

$$\tilde{C}^{(\tau_q)}_{-\frac{N}{2}} = \frac{1}{\sqrt{q}} \sum_{l=0}^{q-1} e^{i\tau_q l^2} \cos^N(\tau_q l), \tag{16a}$$

$$\tilde{C}^{(\tau_q)}_{\frac{N}{2}} = \frac{i^N}{\sqrt{q}} \sum_{l=0}^{q-1} e^{i\tau_q l^2} \sin^N(\tau_q l). \tag{16b}$$

Note that the sine and cosine functions in Eqs. (16), when taken to the power of N, give nonzero values only when they are close to unity, which is for $l = q/2$ and $l = 0$, respectively. For large N, this gives the Bell coefficient as

$$\tilde{\mathcal{E}}_N^{(Q)} \simeq \frac{1}{q^2}, \tag{17}$$

for times τ_q. This is a very simple yet powerful formula allowing us to predict the extent of Bell correlations in various many-body systems. The blue dots in Fig. 1(a) and 1(b) show the agreement between this approximate expression and the exact correlator from Eq. (9) calculated with the coefficients (10a) and (10b).

Hence, as q drops, so that the time grows (recall that $\tau_q = (\pi/q)$), the value of the Bell correlator increases to reach the maximal attainable value $\tilde{\mathcal{E}}_N^{(Q)} = \frac{1}{4}$ at the half of the dynamics period. But there is more information about

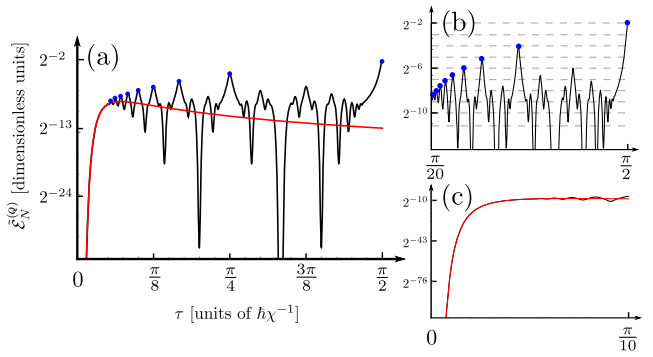

FIG. 1. The Bell correlator $\tilde{\mathcal{E}}_N^{(Q)}$ (black solid line) as a function of χt and for $N = 200$. (a) Compared with the short-times approximate behavior (13) (solid red line) and the long-times solution from Eq. (17) (blue points). (b) The enlargement onto the long-time behavior and the growing depth of Bell correlations signaled with dashed grey lines for $k = N, N-1, \ldots, N-8$ from top to bottom. (c) The focus onto short times up to $\chi t/\hbar = \pi/10$.

the many-body Bell correlations that can be extracted from the expression (17). Namely, when

$$\tilde{\mathcal{E}}_N^{(Q)} > \frac{1}{8}\frac{1}{2^{N-k}}, \tag{18}$$

the correlator can be reproduced with a system of N qubits, where the Bell correlations encompass at least k qubits (in analogy to k-partite entanglement) [40,41]. For instance, when $\tilde{\mathcal{E}}_N^{(Q)} > \frac{1}{8}$, all N qubits are Bell correlated, if $\tilde{\mathcal{E}}_N^{(Q)} > (1/16)$, the Bell correlations extend over at least $N-1$ particles and so on. Note that the correlator from Eq. (5) can also be used to witness the k-partite entanglement in the system [39,40]. Similar to Eq. (5), when

$$\tilde{\mathcal{E}}_N^{(Q)} \leqslant 4^{-N}, \tag{19}$$

the many-body correlator can be reproduced with a fully separable state. The analogy to the k-partite Bell correlations extends further, namely, if

$$\tilde{\mathcal{E}}_N^{(Q)} > \frac{1}{16}\frac{1}{4^{N-k}}, \tag{20}$$

the correlator is consistent with that of a system where k qubits form a k-partite entangled state and the other $N-k$ are separable, just as in Eq. (18).

Since the expression (4), which is used to derive (17) is valid for $\tau_q > \tau_s$, hence, we observe that, at the shortest time when Eq. (17) can be used, it holds that $\tilde{\mathcal{E}}_N^{(Q)} \simeq N^{-\frac{4}{3}}$. For instance, when $N = 10^3$, this gives $\tilde{\mathcal{E}}_N^{(Q)} \simeq 10^{-4}$. Using Eq. (18), we obtain that, in this case, $\tilde{\mathcal{E}}_N^{(Q)} \simeq (1/10^4) > \frac{1}{8}\frac{1}{2^{11}}$. Hence, even at such a short time, the Bell correlations extend over $k = 10^3 - 11 = 989$ particles. Generally speaking, by comparing the value of the correlator at the critical time with Eq. (18), we learn that, at that instant,

$k = N - \frac{4}{3}\log_2 N + 3$ qubits are Bell correlated, encompassing almost the whole system for large N. Thus, we show that the OAT procedure naturally generates many-body Bell correlated states, very early in dynamics when $\tau \gtrsim \tau_{\mathrm{crit}}$, one of the main results of this Letter. In the Supplemental Material [48], we demonstrate that the Bell correlations generated with the OAT are robust to the fluctuations of the number of atoms in the initial state as long as these fluctuations remain close to the shot-noise level.

Next, we illustrate our theory for certification of Bell correlations with OAT in the specific system, namely N ultracold bosonic atoms in a 1D optical lattice with $M = N$ sites, each of mass m in two internal states a and b. The system Hamiltonian reads

$$\hat{H} = \hat{H}_a + \hat{H}_b + \hat{H}_{ab}, \tag{21}$$

where

$$\hat{H}_a = -J\sum_j (\hat{a}_j^\dagger \hat{a}_{j+1} + \mathrm{H.c.}) + \frac{U_{aa}}{2}\sum_j \hat{n}_{a,j}(\hat{n}_{a,j} - 1), \tag{22}$$

describes nearest-neighbor tunneling and repulsive interaction as for the Bose-Hubbard model (BHM), and analogically for $\hat{H}_b$, while $\hat{H}_{ab} = U_{ab}\sum_j \hat{n}_{a,j}\hat{n}_{b,j}$. Here, $\hat{a}_j$ is the annihilation operator of the atom at the jth lattice site in mode a, and $\hat{n}_{a,j}$ is the corresponding particle number operator. We assume the optical lattice is formed by a standing laser beam with wave-vector $k_{\mathrm{latt}} = 2\pi/\lambda$, where the optical lattice wavelength is $\lambda = 2d$, d is the distance between neighboring sites. The height of the optical lattice V_0 determines the coupling parameters, i.e., hopping amplitude $J = 4/\sqrt{\pi} V_0^{3/4} e^{-2\sqrt{V_0}}$, and contact interaction amplitudes $U_{\alpha\alpha'} = \sqrt{8/\pi} a_{\alpha\alpha'} V_0^{1/4}$, with $a_{\alpha\alpha'}$ being the scattering lengths. We consider parameters used in [25] which can be realized in current experiments, it is $V_0/E_R = 0.3$, $J/U_{aa} \approx 3$ and $U_{aa} = U_{bb}$, $U_{ab} = 0.95U$. The collective spin operators can be defined through $\hat{J}_+ = \sum_{j=1}^M \hat{a}_j^\dagger \hat{b}_j$, $\hat{J}_- = \sum_{j=1}^M \hat{b}_j^\dagger \hat{a}_j$, and $\hat{J}_x = (\hat{J}_+ + \hat{J}_-)/2$, $\hat{J}_y = (\hat{J}_+ - \hat{J}_-)/(2i)$, $\hat{J}_z = (\hat{N}_a - \hat{N}_b)/2$ where $\hat{N}_{a/b}$ is the operator of the number of atoms in the state a/b.

The OAT model can be simulated with the BHM (21) in the superfluid phase when the condensate fraction is close to one [23,25]. To see this, we consider (21) in the Fourier space, by using $\hat{a}_j = (1/\sqrt{M})\sum_{q_n} e^{-ix_j q_n}\hat{a}_{q_n}$ with $q_n = (2\pi/N)n$ and $n = 0, \pm 1, \pm 2, \ldots$, is an integer (and analogically for $\hat{b}_j$). Next, when atoms microscopically occupy the zero momentum mode $q_n = 0$, the system Hamiltonian considered for zero quasimomentum mode $q_n = 0$ reduces to the OAT model,

$$\hat{H} \approx \chi \hat{J}^2_{z,q_n=0}, \tag{23}$$

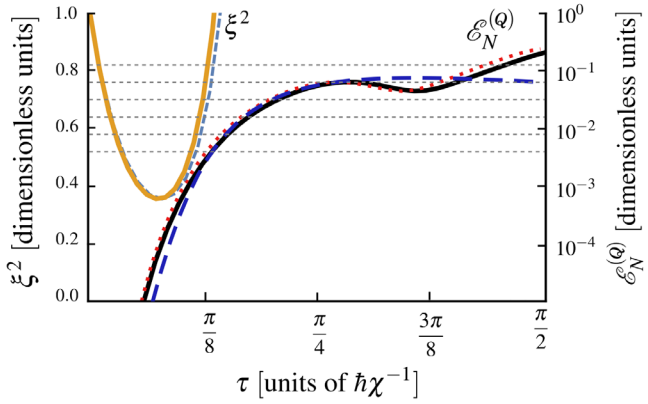

FIG. 2. The Bell correlator $\tilde{\mathcal{E}}_N^{(Q)}$ (the three curves and the vertical scale in the right part of the plot) and the spin-squeezing parameter ξ^2 (the two curves and the vertical scale on the left) for $N = 8$. For $\tilde{\mathcal{E}}_N^{(Q)}$: the solid black line is the correlator from Eq. (9), for the two-component BHM (21) when the system is in the superfluid phase. The dotted red curve is obtained for the OAT model, see Eq. (23), while the dashed blue curve shows the result of the short-times approximation (13). Particular bounds for the k-qubit Bell correlations (18) are marked by the dashed grey lines for $k = 8, 7, \ldots, 3$ from top to bottom. For ξ^2: the squeezing parameter (3) is marked by the solid orange line (exact numerical results for BHM), while the dashed blue line is calculated with the OAT (23).

when omitting constant energy terms, and where $\chi = [(U - U_{ab})/M]$ gives the relevant timescale (for the derivation, see Supplemental Material [48]). Note here, the resulting critical time is independent of the total number of atoms $t_{\mathrm{crit}} = \tau_{\mathrm{crit}}\hbar/\chi \approx \hbar/(U - U_{ab})$ when $M = N$, as considered here.

We performed many-body numerical calculations [54], to prepare the initial spin coherent state given by the symmetric superposition of atoms in states a and b, to evaluate the unitary evolution and calculate the spin squeezing parameter (3) and the Bell correlator (5). In Fig. 2, we show results for $N = 8$ atoms. One can clearly see the overall agreement between the Bose-Hubbard (solid lines) and OAT (closed points) models. However, an analysis of the evolution of $\tilde{\mathcal{E}}_N^{(Q)}$ brings interesting conclusions. The lower bound of $\tilde{\mathcal{E}}_{N=8}^{(Q)} \approx 4 \times 10^{-3}$ is marked in Fig. 2, and Bell correlations emerge for times $\tau_{\mathrm{crit}} \approx \pi/8$ according to (15). We can see that, around this time, the states are spin squeezed as $\xi^2 < 1$ (marked by the orange line) what suggests that there are already nontrivial two-body correlations in the system.

In the subsequent moments of time, Bell correlations start to extend over at least three atoms, and the next four atoms when $\tilde{\mathcal{E}}_{N=8}^{(Q)} \gtrsim 7.8 \times 10^{-3}$, five atoms when $\tilde{\mathcal{E}}_{N=8}^{(Q)} \gtrsim 1.5 \times 10^{-2}$, etc., and over all eight atoms when $\tilde{\mathcal{E}}_{N=8}^{(Q)} \gtrsim 0.125$. Finally, let us comment on the entanglement depth given by (19), i.e., $\tilde{\mathcal{E}}_{N=8}^{(Q)} \gtrsim 1.5 \times 10^{-5}$, which is

surpassed for $\tau \approx \pi/20$. According to Eq. (20), when $\tilde{\mathcal{E}}^{(Q)}_{N=8} \gtrsim 2 \times 10^{-4}$ the entanglement extends over four atoms. Finally, when $\tilde{\mathcal{E}}^{(Q)}_{N=8} > 1/16$ entanglement extends over the whole system.

In this Letter, we presented a systematic analytical study of the creation of many-body Bell-correlated states generated during one-axis twisting dynamics in two-component bosonic systems. We identified the critical time at which the many-body Bell correlations emerge and derived a simple and powerful formula allowing us to characterize the Bell correlations- and entanglement-depth at later times. We applied these findings to classify the generation of many-body Bell correlations in systems of two-component bosons loaded into a one-dimensional optical lattice. We showed that our analytical findings are in very good agreement with the full many-body numerical calculations.

The experimental verification of our findings requires access to many-body quantum correlation functions. A remarkable progress in experimental advances in the control of many-body quantum systems allows measurement of correlation functions up to sixth order [55], second Rényi entropy for $N = 4$ [56], and $N = 5$ particles [57] via extraction characteristic of a quantum state using a controlled-swap gate acting on two copies of the state [58], and for $N = 10$ particles [59] via randomized measurements technique [60–65]. However, for the indistinguishable particles considered here, the measurement of the proposed many-body correlator still presents an experimental challenge for $N \geq 6$ atoms. The future research direction would be to consider single addressable particles, like trapped ions, and consider the generation and detection of many-body Bell correlations in noisy intermediate-scale quantum devices.

Our study contributes to the dynamically emerging field of quantum technologies having both fundamental and practical aspects.

E. W. acknowledges the support of the Polish National Science Centre through the project MAQS under QuantERA, which has received funding from the European Union's Horizon 2020 research and innovation program under Grant Agreement No. 731473, Project No. 2019/32/Z/ST2/00016. J. C. was funded by the National Science Centre, Poland, within the QuantERA II Programme that has received funding from the European Union's Horizon 2020 research and innovation programme under Grant Agreement No. 101017733, Project No. 2021/03/Y/ST2/00195. M. P. acknowledges the support of the Polish National Agency for Academic Exchange, the Bekker Programme No. PPN/BEK/2020/1/00317, and the computer resources at MareNostrum and the technical support provided by BSC (Grant No. RES-FI-2022-1-0042). ICFO group acknowledges support from: ERC AdG NOQIA; Ministerio de Ciencia y Innovation Agencia Estatal de Investigaciones (PGC2018-097027-B-I00/10.13039/501100011033, CEX2019-000910-S/10.13039/501100011033, Plan National FIDEUA PID2019-106901GB-I00, FPI, QUANTERA MAQS PCI2019-111828-2, QUANTERA DYNAMITE PCI2022-132919, Proyectos de I + D + I "Retos Colaboración" QUSPIN RTC2019-007196-7); MCIN Recovery, Transformation and Resilience Plan with funding from European Union NextGenerationEU (PRTR C17.I1); Fundació Cellex; Fundació Mir-Puig; Generalitat de Catalunya (European Social Fund FEDER and CERCA program (AGAUR Grant No. 2017 SGR 134, QuantumCAT\U16-011424, co-funded by ERDF Operational Program of Catalonia 2014-2020); Barcelona Supercomputing Center MareNostrum (FI-2022-1-0042); EU Horizon 2020 FET-OPEN OPTOlogic (Grant No 899794); National Science Centre, Poland (Symfonia Grant No. 2016/20/W/ST4/00314); European Union's Horizon 2020 research and innovation programme under the Marie-Skłodowska-Curie Grant Agreement No. 101029393 (STREDCH) and No 847648 ("La Caixa" Junior Leaders fellowships ID100010434: LCF/BQ/PI19/11690013, LCF/BQ/PI20/11760031, LCF/BQ/PR20/11770012, LCF/BQ/PR21/11840013).

*Corresponding author.
marcin.plodzien@icfo.eu

[1] A. Acín, I. Bloch, H. Buhrman, T. Calarco, C. Eichler, J. Eisert, D. Esteve, N. Gisin, S. J. Glaser, F. Jelezko, S. Kuhr, M. Lewenstein, M. F. Riedel, P. O. Schmidt, R. Thew, A. Wallraff, I. Walmsley, and F. K. Wilhelm, New J. Phys. **20**, 080201 (2018).
[2] J. Eisert, D. Hangleiter, N. Walk, I. Roth, D. Markham, R. Parekh, U. Chabaud, and E. Kashefi, Nat. Rev. Phys. **2**, 382 (2020).
[3] A. Kinos, D. Hunger, R. Kolesov, K. Mølmer, H. de Riedmatten, P. Goldner, A. Tallaire, L. Morvan, P. Berger, S. Welinski, K. Karrai, L. Rippe, S. Kröll, and A. Walther, arXiv:2103.15743.
[4] A. Laucht *et al.*, Nanotechnology **32**, 162003 (2021).
[5] C. Becher, W. Gao, S. Kar, C. Marciniak, T. Monz, J. G. Bartholomew, P. Goldner, H. Loh, E. Marcellina, K. E. J. Goh, T. S. Koh, B. Weber, Z. Mu, J.-Y. Tsai, Q. Yan, S. Gyger, S. Steinhauer, and V. Zwiller, arXiv:2202.07309.
[6] J. Fraxanet, T. Salamon, and M. Lewenstein, arXiv:2204.08905.
[7] D. J. Wineland, J. J. Bollinger, W. M. Itano, F. L. Moore, and D. J. Heinzen, Phys. Rev. A **46**, R6797 (1992).
[8] M. Kitagawa and M. Ueda, Phys. Rev. A **47**, 5138 (1993).
[9] K. Gietka, P. Szańkowski, T. Wasak, and J. Chwedeńczuk, Phys. Rev. A **92**, 043622 (2015).
[10] Y. Li, Y. Castin, and A. Sinatra, Phys. Rev. Lett. **100**, 210401 (2008).
[11] Y. Li, P. Treutlein, J. Reichel, and A. Sinatra, Eur. Phys. J. B **68**, 365 (2009).
[12] M. Wang, W. Qu, P. Li, H. Bao, V. Vuletić, and Y. Xiao, Phys. Rev. A **96**, 013823 (2017).
[13] D. Kajtoch, E. Witkowska, and A. Sinatra, Phys. Rev. A **98**, 023621 (2018).

[14] M. Schulte, C. Lisdat, P. O. Schmidt, U. Sterr, and K. Hammerer, Nat. Commun. **11**, 5955 (2020).

[15] K. Gietka, A. Usui, J. Deng, and T. Busch, Phys. Rev. Lett. **126**, 160402 (2021).

[16] T. Comparin, F. Mezzacapo, and T. Roscilde, Phys. Rev. A **105**, 022625 (2022).

[17] M. F. Riedel, P. Böhi, Y. Li, T. W. Hänsch, A. Sinatra, and P. Treutlein, Nature (London) **464**, 1170 (2010).

[18] C. Gross, T. Zibold, E. Nicklas, J. Estève, and M. K. Oberthaler, Nature (London) **464**, 1165 (2010).

[19] C. D. Hamley, C. S. Gerving, T. M. Hoang, E. M. Bookjans, and M. S. Chapman, Nat. Phys. **8**, 305 (2012).

[20] A. Qu, B. Evrard, J. Dalibard, and F. Gerbier, Phys. Rev. Lett. **125**, 033401 (2020).

[21] I. D. Leroux, M. H. Schleier-Smith, and V. Vuletić, Phys. Rev. Lett. **104**, 073602 (2010).

[22] K. Maussang, G. E. Marti, T. Schneider, P. Treutlein, Y. Li, A. Sinatra, R. Long, J. Estève, and J. Reichel, Phys. Rev. Lett. **105**, 080403 (2010).

[23] D. Kajtoch, E. Witkowska, and A. Sinatra, Europhys. Lett. **123**, 20012 (2018).

[24] P. He, M. A. Perlin, S. R. Muleady, R. J. Lewis-Swan, R. B. Hutson, J. Ye, and A. M. Rey, Phys. Rev. Res. **1**, 033075 (2019).

[25] M. Płodzień, M. Kościelski, E. Witkowska, and A. Sinatra, Phys. Rev. A **102**, 013328 (2020).

[26] M. Mamaev, I. Kimchi, R. M. Nandkishore, and A. M. Rey, Phys. Rev. Res. **3**, 013178 (2021).

[27] T. Hernández Yanes, M. Płodzień, M. Mackoit Sinkevičienė, G. Žlabys, G. Juzeliūnas, and E. Witkowska, Phys. Rev. Lett. **129**, 090403 (2022).

[28] M. Dziurawiec, T. H. Yanes, M. Płodzień, M. Gajda, M. Lewenstein, and E. Witkowska, arXiv:2208.04019.

[29] J. Tura, R. Augusiak, A. B. Sainz, T. Vértesi, M. Lewenstein, and A. Acín, Science **344**, 1256 (2014).

[30] R. Schmied, J.-D. Bancal, B. Allard, M. Fadel, V. Scarani, P. Treutlein, and N. Sangouard, Science **352**, 441 (2016).

[31] A. Aloy, J. Tura, F. Baccari, A. Acín, M. Lewenstein, and R. Augusiak, Phys. Rev. Lett. **123**, 100507 (2019).

[32] F. Baccari, J. Tura, M. Fadel, A. Aloy, J.-D. Bancal, N. Sangouard, M. Lewenstein, A. Acín, and R. Augusiak, Phys. Rev. A **100**, 022121 (2019).

[33] J. Tura, A. Aloy, F. Baccari, A. Acín, M. Lewenstein, and R. Augusiak, Phys. Rev. A **100**, 032307 (2019).

[34] G. Müller-Rigat, A. Aloy, M. Lewenstein, and I. Frérot, PRX Quantum **2**, 030329 (2021).

[35] The notion of k producibility of nonlocality is used in the context of assessing the number of particles sharing genuinely nonlocal correlations in a multipartite system.

[36] M. Żukowski and Č. Brukner, Phys. Rev. Lett. **88**, 210401 (2002).

[37] E. G. Cavalcanti, C. J. Foster, M. D. Reid, and P. D. Drummond, Phys. Rev. Lett. **99**, 210405 (2007).

[38] Q. Y. He, P. D. Drummond, and M. D. Reid, Phys. Rev. A **83**, 032120 (2011).

[39] E. G. Cavalcanti, Q. Y. He, M. D. Reid, and H. M. Wiseman, Phys. Rev. A **84**, 032115 (2011).

[40] A. Niezgoda, M. Panfil, and J. Chwedeńczuk, Phys. Rev. A **102**, 042206 (2020).

[41] A. Niezgoda and J. Chwedeńczuk, Phys. Rev. Lett. **126**, 210506 (2021).

[42] J. Chwedenczuk, SciPost Phys. Core **5**, 25 (2022).

[43] The system we consider can be viewed as an ensemble of N indistinguishable qubits. These qubits cannot be addressed individually as spins in chains or optical lattices with one two-level atom per site. The operators addressing individual qubits are absorbed in the collective operators.

[44] Y. Baamara, A. Sinatra, and M. Gessner, arXiv:2112.01786.

[45] D. J. Wineland, J. J. Bollinger, W. M. Itano, and D. J. Heinzen, Phys. Rev. A **50**, 67 (1994).

[46] G. Ferrini, A. Minguzzi, and F. W. J. Hekking, Phys. Rev. A **78**, 023606 (2008).

[47] D. Spehner, K. Pawlowski, G. Ferrini, and A. Minguzzi, Eur. Phys. J. B **87**, 157 (2014).

[48] See Supplemental Material at http://link.aps.org/supplemental/10.1103/PhysRevLett.129.250402 for details which include Refs. [37–39,42] in Sec. I, [25,49] in Sec. II, [7,50] in Sec. III, and [30] in Sec. IV.

[49] D. Kajtoch, E. Witkowska, and A. Sinatra, Phys. Rev. A **98**, 023621 (2018).

[50] D. J. Wineland, J. J. Bollinger, W. M. Itano, and D. J. Heinzen, Phys. Rev. A **50**, 67 (1994).

[51] The matrix element of the Wigner matrix is $d^j_{nm}(\theta)=\langle n|e^{-i\theta\hat{J}_y}|m\rangle=\sqrt{[(j+m)!(j-m)!/(j+n)!(j-n)!]}\,[\sin(\theta/2)]^{m-n}[\cos(\theta/2)]^{m+n}$, with $j=(N/2)$.

[52] A variation of the Bell correlator (13) in time exhibits a single maximum. Here, we are interested in the growth of $\tilde{\mathcal{E}}_N^{(q)}$ for short times which is determined by the exponent in (13). The very short time variation of the Bell correlator can be well approximated by $4e^{-[\pi^2 N/8(1+\kappa^2)]}$ which gives (15).

[53] L. Mandel and E. Wolf, *Optical Coherence and Quantum Optics* (Cambridge University Press, Cambridge, England, 1995).

[54] We employ a standard density matrix renormalization group (DMRG) technique for calculating the initial spin coherent state [66–70]. Time evolution was prepared within an algorithm for time evolution where a one-site time-dependent variational principle (TDVP) scheme [71–74] is combined with a global basis expansion [75]. To perform both DMRG and time evolution, we use ITensor C++ library [76], where we employ the codes for modified TDVP provided by the authors of [75].

[55] R. G. Dall, A. G. Manning, S. S. Hodgman, W. RuGway, K. V. Kheruntsyan, and A. G. Truscott, Nat. Phys. **9**, 341 (2013).

[56] R. Islam, R. Ma, P. M. Preiss, M. Eric Tai, A. Lukin, M. Rispoli, and M. Greiner, Nature (London) **528**, 77 (2015).

[57] N. M. Linke, S. Johri, C. Figgatt, K. A. Landsman, A. Y. Matsuura, and C. Monroe, Phys. Rev. A **98**, 052334 (2018).

[58] A. K. Ekert, C. M. Alves, D. K. L. Oi, M. Horodecki, P. Horodecki, and L. C. Kwek, Phys. Rev. Lett. **88**, 217901 (2002).

[59] T. Brydges, A. Elben, P. Jurcevic, B. Vermersch, C. Maier, B. P. Lanyon, P. Zoller, R. Blatt, and C. F. Roos, Science **364**, 260 (2019).

[60] B. Vermersch, A. Elben, M. Dalmonte, J. I. Cirac, and P. Zoller, Phys. Rev. A **97**, 023604 (2018).

[61] A. Elben, B. Vermersch, C. F. Roos, and P. Zoller, Phys. Rev. A **99**, 052323 (2019).
[62] A. Elben, J. Yu, G. Zhu, M. Hafezi, F. Pollmann, P. Zoller, and B. Vermersch, Sci. Adv. **6**, eaaz3666 (2020).
[63] A. Elben, R. Kueng, H. Y. R. Huang, R. van Bijnen, C. Kokail, M. Dalmonte, P. Calabrese, B. Kraus, J. Preskill, P. Zoller, and B. Vermersch, Phys. Rev. Lett. **125**, 200501 (2020).
[64] A. Rath, C. Branciard, A. Minguzzi, and B. Vermersch, Phys. Rev. Lett. **127**, 260501 (2021).
[65] A. Elben, S. T. Flammia, H.-Y. Huang, R. Kueng, J. Preskill, B. Vermersch, and P. Zoller, The randomized measurement toolbox (2022).
[66] S. R. White, Phys. Rev. Lett. **69**, 2863 (1992).
[67] S. R. White, Phys. Rev. B **48**, 10345 (1993).
[68] U. Schollwöck, Rev. Mod. Phys. **77**, 259 (2005).
[69] U. Schollwöck, Ann. Phys. (Amsterdam) **326**, 96 (2011), January 2011 Special Issue.
[70] R. Orús, Ann. Phys. (Amsterdam) **349**, 117 (2014).
[71] P. Kramer, J. Phys. **99**, 012009 (2008).
[72] J. Haegeman, J. I. Cirac, T. J. Osborne, I. Pižorn, H. Verschelde, and F. Verstraete, Phys. Rev. Lett. **107**, 070601 (2011).
[73] T. Koffel, M. Lewenstein, and L. Tagliacozzo, Phys. Rev. Lett. **109**, 267203 (2012).
[74] J. Haegeman, C. Lubich, I. Oseledets, B. Vandereycken, and F. Verstraete, Phys. Rev. B **94**, 165116 (2016).
[75] M. Yang and S. R. White, Phys. Rev. B **102**, 094315 (2020).
[76] M. Fishman, S. R. White, and E. M. Stoudenmire, arXiv: 2007.14822.